Thermoelectricity at nanoscale: theoretical models

Dima Shepelyansky (CNRS, Toulouse)
www.quantware.ups-tlse.fr/dima

Joint work with Oleg Zhirov (BINP) Europhys. Lett. **103**, 68008 (2013)

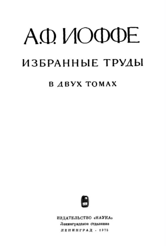

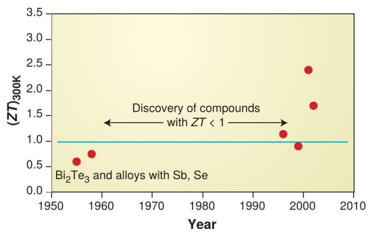

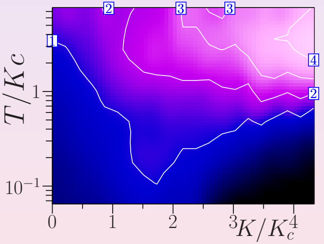

Time evolution of figure of merit *ZT* (center)
(from A.Majumdar Science **303**, 777 (2004))

Early works

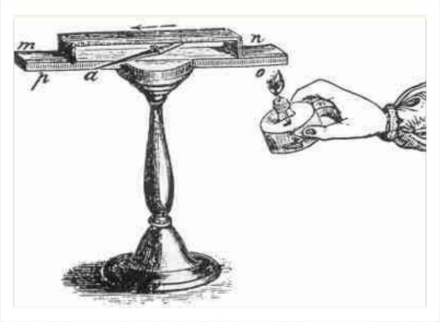

T. Seebeck-deflection of a compass needle (circa 1823)

from Y.Imry (Weizmann Inst) talk at Inst. H. Poincaré, Paris (2012)

Early works

A. F. Ioffe

semiconductors

and figure of merit

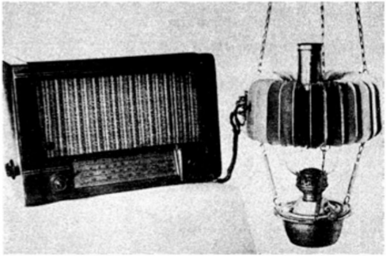

Oil burning lamp powering a radio using the first commercial thermoelectric generator containing ZnSb built in USSR, circa 1948

from Y.Imry (Weizmann Inst) talk at Inst. H. Poincaré, Paris (2012)

Main characteristics

Seebeck coefficient:

$S = \Delta V/\Delta T = \pi^2 {k_B}^2 T[(d \ln \sigma/dE)]|_{E_F}/e$ (Mott relation (1958))

For 2DEG with Wiedemann-Franz law: $S = 2\pi {k_B}^2 Tm/(3eh^2 n_e)$;

typical value $S \approx 10\mu V/K$ at $T = 0.3K$, $n_e = 4 \cdot 10^{10} cm^{-2}$

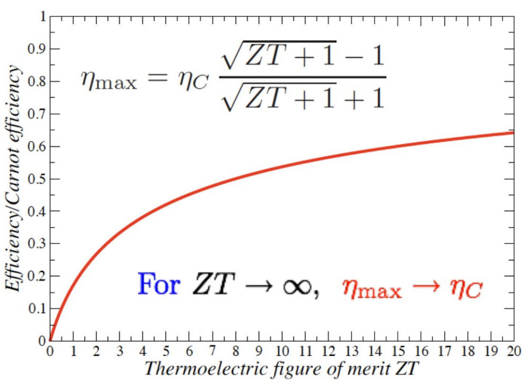

Thermoelectric figure of merit $ZT = \sigma S^2 T/\kappa$,

thermal conductivity $\kappa = \kappa_{el} + \kappa_{phonon}$ (heat flux $Q = -\kappa \nabla T$)

Experiments on Seebeck coefficient for 2DEG

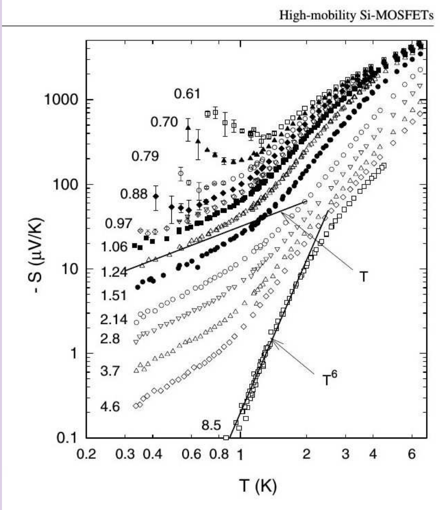

Figure 4. The thermopower S for sample 1 at various fixed electron densities n (in units of 10^{15} m^{-2}) as a function of temperature.

R.Fletcher, V.M.Pudalov et al. Semicond. Sci. Technol. **15**, 386 (2001)

Experiments on Seebeck coefficient for 2DEG

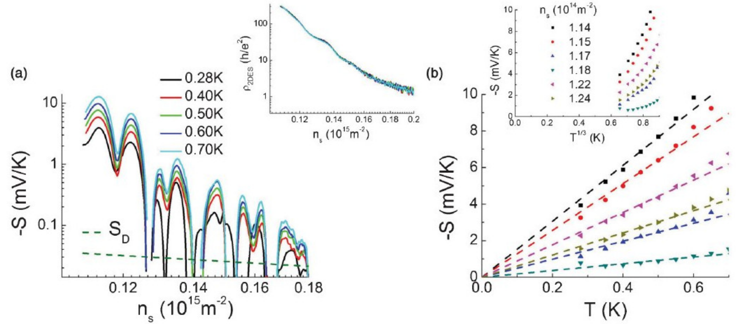

FIG. 5. (Color online) (a) S vs n_s for 0.28 K $< T <$ 0.7 K. The broken green line shows S_d [Eq. (2)] at 0.28 K. Inset: ρ_{2DES} vs n_s at the same T values; there is little T dependence in this range. (b) Low-T linear variation of S. Inset: Descriptions based on variable-ranged hopping, where S is expected to decay to zero as $T^{1/3}$, do not adequately describe the observed data.

V.Narayan, S.Goswami, M.Pepper et al. PRB **85**, 125406 (2012)

In dimensionless units $S = 10mV/K \approx 100 \gg 1$

ZT in various materials

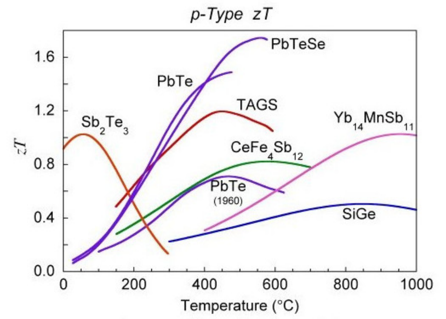

zT for p-type thermoelectric materials

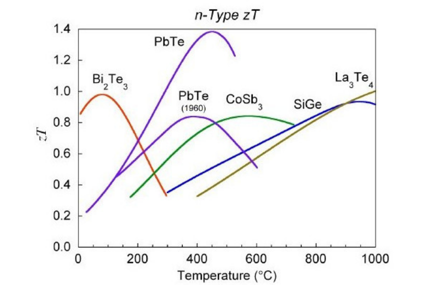

zT for n-type thermoelectric materials

G. Jeffrey Snyder and Eric S. Toberer "Complex Thermoelectric Materials" Nature Materials 7, 105-114 (2008).

from http://www.thermoelectrics.caltech.edu/thermoelectrics/

ZT in p-type Bi_2Te_3/Sb_2Te_3 superlattices

Phonon-blocking/electron-transmitting structures

The results obtained with the 10Å/50Å Bi_2Te_3/Sb_2Te_3 superlattices indicate that we can fine-tune the phonon and hole (charge carriers)

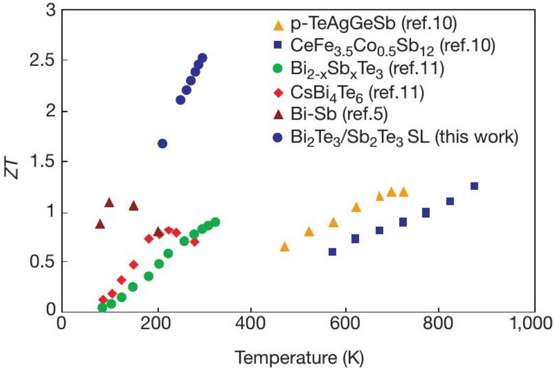

Figure 3 Temperature dependence of ZT of 10Å/50Å p-type Bi_2Te_3/Sb_2Te_3 superlattice compared to those of several recently reported materials.

R.Venkatasubramanian et al. (N.Carolina) Nature **413**, 597 (2001)

ZT in *SnSe*

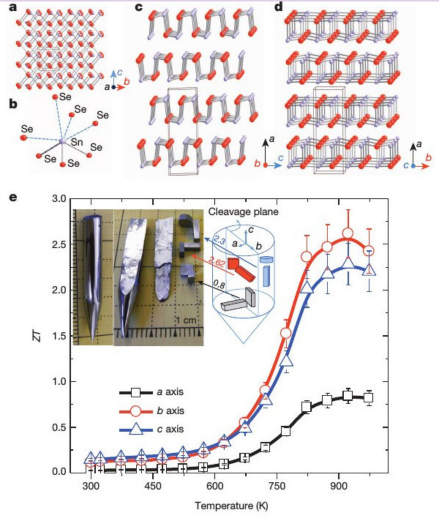

Figure 1 | SnSe crystal structure *Pnma* and *ZT* values. a, Crystal structure along the *a* axis: grey, Sn atoms; red, Se atoms. **b**, Highly distorted $SnSe_7$ coordination polyhedron with three short and four long Sn–Se bonds. **c**, Structure along the *b* axis. **d**, Structure along the *c* axis. **e**, Main panel, *ZT* values along different axial directions; the *ZT* measurement uncertainty is about 15% (error bars). Inset images: left, a typical crystal; right, a crystal cleaved along the (l00) plane, and specimens cut along the three axes and corresponding measurement directions. Inset diagram, how crystals were cut for directional measurements; *ZT* values are shown on the blue, red and grey arrows; colours represent specimens oriented in different directions.

Li-Dong Zhao et al. (Illinois) Nature **508**, 373 (2014)

Research at CNRS Grenoble (O.Bourgeois Refs.3,4)

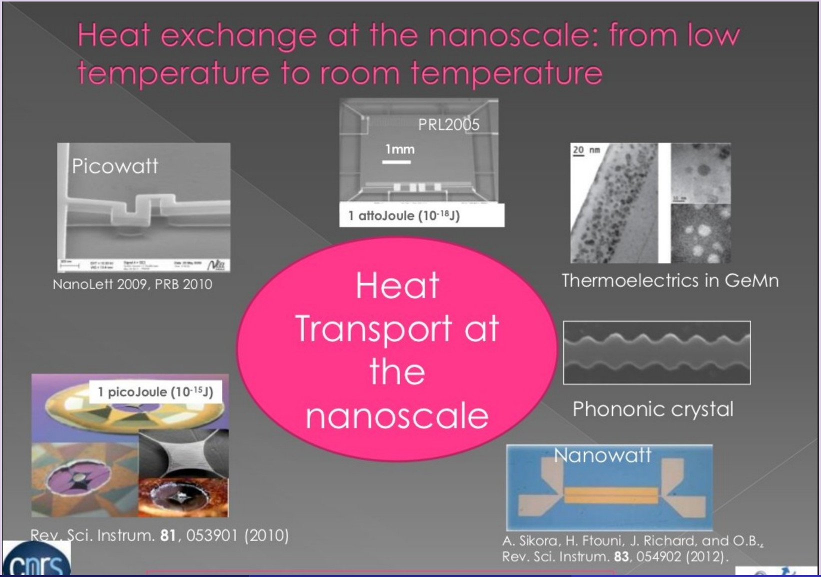

Applications

TE Applications are mostly 'Niche' Applications

-Laser, PCR

CITIZEN
Eco-Drive Thermo
Watch

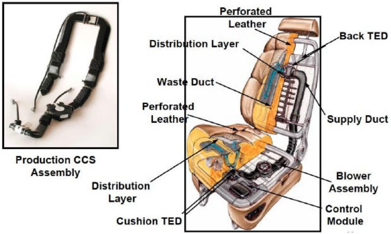

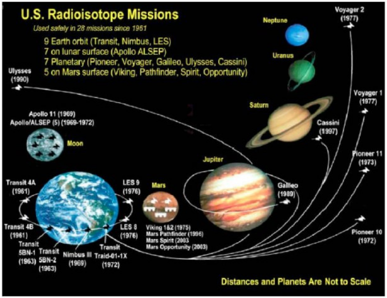

Thermoelectricity of Wigner crystal in a periodic potential

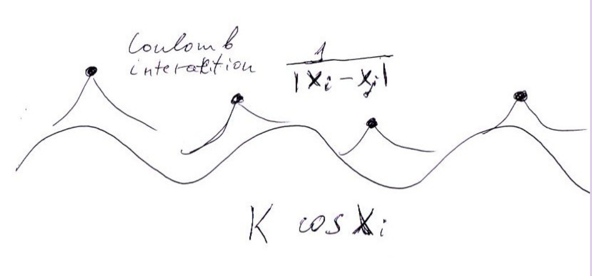

Hamiltonian $H = \sum_i \left(\frac{p_i^2}{2} + K \cos x_i + \frac{1}{2} \sum_{j \neq i} \frac{1}{|x_i - x_j|} \right)$

Dynamic equations $\dot{p}_i = -\partial H / \partial x_i + E_{dc} - \eta p_i + g \xi_i(t)$, $\dot{x}_i = p_i$

Here the Langevin force is given by $g = \sqrt{2\eta T}$, $\langle \xi_i(t) \xi_j(t') \rangle = \delta_{ij} \delta(t - t')$;
$n_e = \nu / 2\pi$, $\nu = \nu_g = 1.618...$ Fibonacci rational approximates.

Aubry transition at $K = K_c = 0.0462$.
I.Garcia-Mata, O.Zhirov, DLS EPJD **41**, 325 (2007)

Time evolution of Wigner crystal

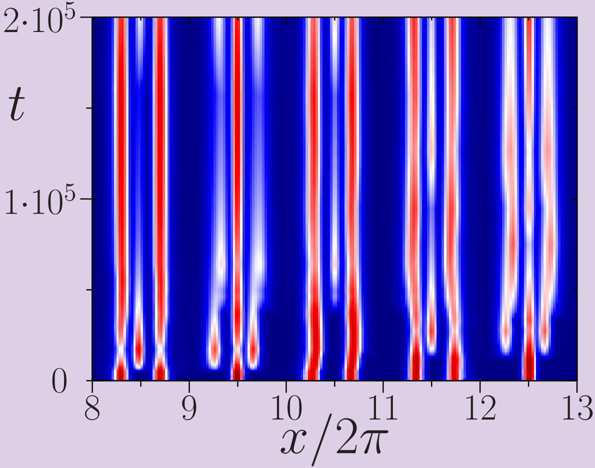

Electron density variation in space and time from one Langevin trajectory at $K/K_c = 2.6$, $T/K_c = 0.11$, $\eta = 0.02$, $N = 34$, $M = L/2\pi = 21$; density changes from zero (dark blue) to maximal density (dark red); only a fragment of x space is shown.

Numerical fits

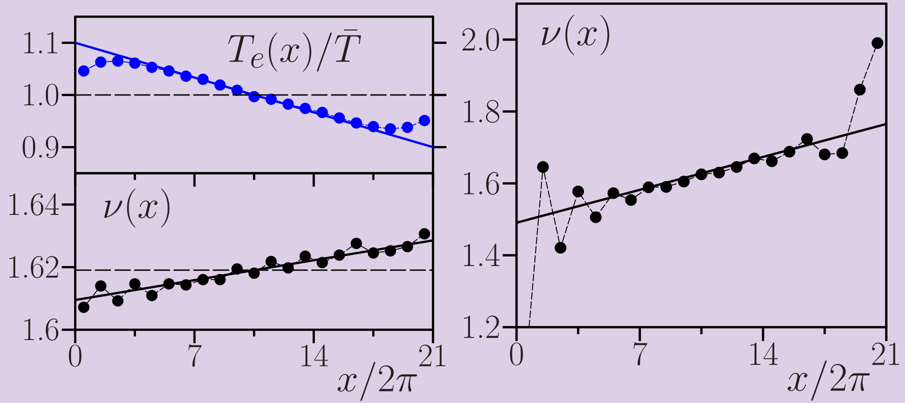

Left panels: dependence of electron temperature $T_e(x)$ *(top, blue points)* and rescaled density $\nu(x)$ *(bottom, black points)* on distance x along the chain placed on the Langevin substrate with a constant temperature gradient (it is shown by the blue line) at average temperature $\bar{T} = 0.01$ and temperature difference $\Delta T = 0.2\bar{T}$; black line shows the fit of density variation in the bulk part of the sample. *Right panel*: density variation produced by a static electric field $E_{dc} = 4 \times 10^{-4}$ at a constant substrate temperature $T = 0.01$; black line shows the fit of gradient in the bulk part of the sample. Here $N = 34$, $M = 21$, $K = 1.52K_c$, $\eta = 0.02$, averaging is done over time interval $t = 10^7$; $S = 3.3$ at $T = 0.01 \approx 0.22K_c$.

Seebeck coefficient

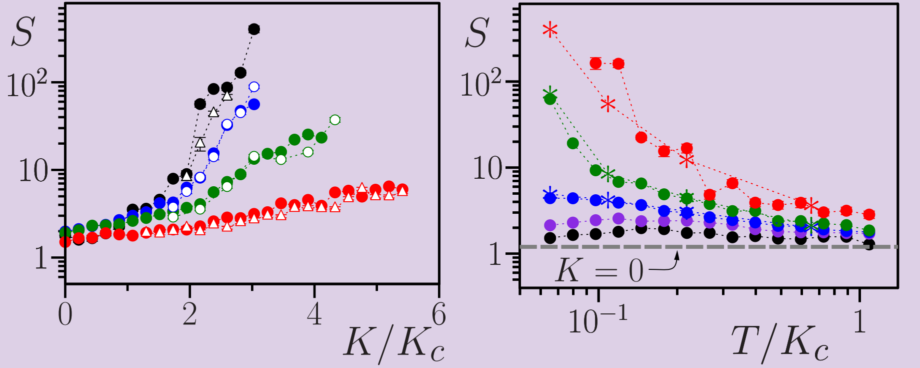

Left panel: Dependence of the Seebeck coefficient S on rescaled potential amplitude K/K_c at temperatures $T/K_c = 0.065, 0.11, 0.22$ and 0.65 shown by black, blue, green and red colors, respectively from top to bottom. The full and open symbols correspond respectively to chains with $N = 34$, $M = 21$ and $N = 55$, $M = 34$. *Right panel*: Dependence of S on T/K_c at different $K/K_c = 0, 0.75, 1.5, 2.2, 3$ shown respectively by black, violet, blue, green and red points; $N = 34$, $M = 21$; the dashed gray line shows the case $K = 0$ for noninteracting particles. The stars show corresponding results from left plane at same N, M. Dotted curves are drown to adapt an eye. Here and in other Figs. the statistical error bars are shown when they are larger than the symbol size. Here $\eta = 0.02$.

Conductivity and thermal conductivity

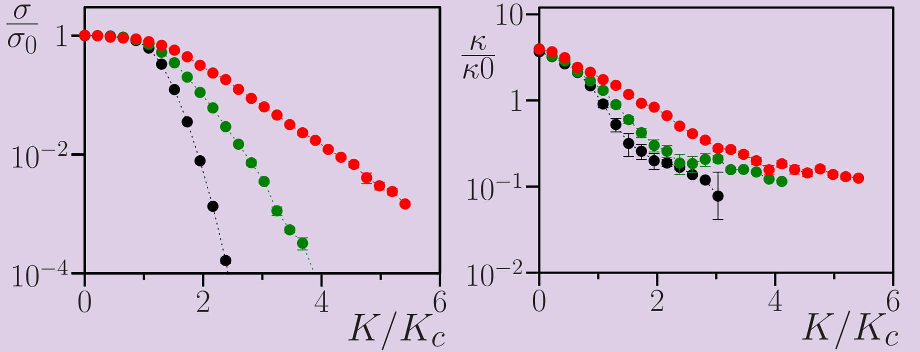

Left panel: Rescaled electron conductivity σ/σ_0 as a function of K/K_c shown at rescaled temperatures $T/K_c = 0.065, 0.22, 0.65$ by black, green and red points respectively. *Right panel*: Rescaled thermal conductivity κ/κ_0 as a function of K/K_c shown at same temperatures and colors as in left panel. Here we have $N = 34$, $M = 21$, $\eta = 0.02$, $\sigma_0 = \nu_g/(2\pi\eta)$, $\kappa_0 = \sigma_0 K_c$.

ZT dependence on parameters

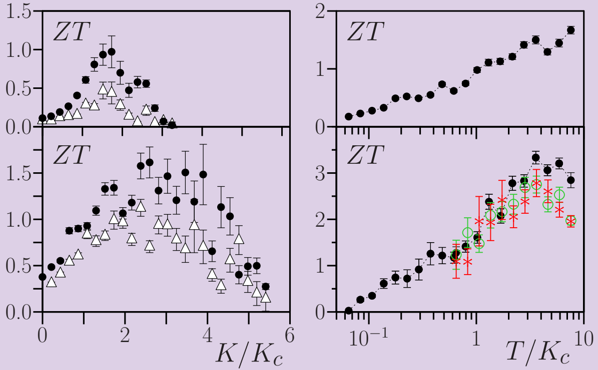

Left panels: Dependence of ZT on K/K_c at temperatures $T/K_c = 0.11$ (top panel) and $T/K_c = 0.65$ (bottom panel); the black points and open triangles correspond respectively to $\eta = 0.02$ and $\eta = 0.05$ at $N = 34$, $M = 21$. *Right panels*: Dependence of ZT on T/K_c for $K/K_c = 0.75$ at $\eta = 0.02$, $N = 34$, $M = 21$. *Bottom right panel*: Same as in top right panel at $K/K_c = 2.6$ and $N = 34$, $M = 21$ (black points); $N = 89$, $M = 55$ (green circles); $N = 144$, $M = 89$ (red stars).

ZT dependence on parameters

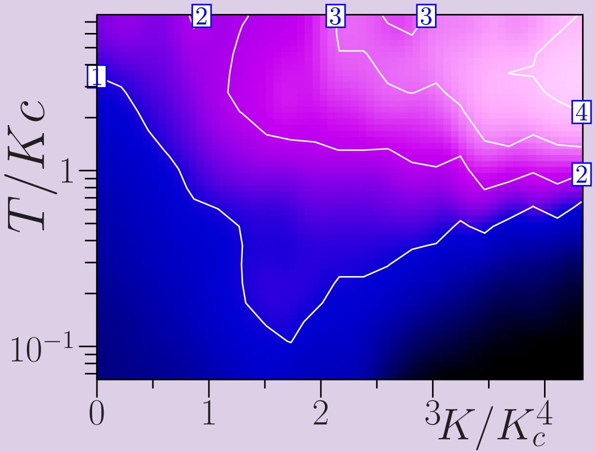

Dependence of ZT on K/K_c and T/K_c shown by color changing from $ZT = 0$ (black) to maximal $ZT = 4.5$ (light rose); contour curves show values $ZT = 1, 2, 3, 4$. Here $\eta = 0.02$, $N = 34$, $M = 21$.

Other quantities dependences

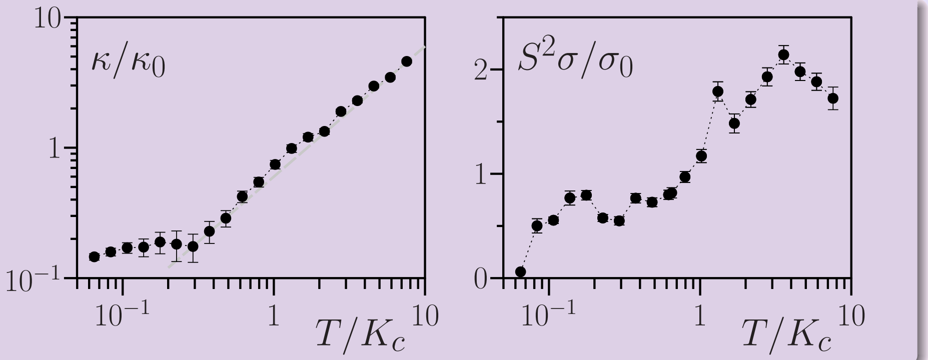

Left panel: Rescaled thermal conductivity κ/κ_0 as a function of rescaler temperature T/K_c, to adapt an eye the straight dashed line shows the dependence $\kappa/\kappa_0 = 0.6T/K_c$; *right panel*: same as in left panel for $S^2\sigma/\sigma_0$. Data are obtained at $K/K_c = 2.6$, $\eta = 0.02$, $N = 34$, $M = 21$, $\sigma_0 = \nu_g/(2\pi\eta)$, $\kappa_0 = \sigma_0 K_c$.

Physical parameters

In physical units we can estimate the critical potential amplitude as $U_c = K_c e^2/(\epsilon d)$, where ϵ is a dielectric constant, Δx is a lattice period and $d = \nu \Delta x/2\pi$ is a rescaled lattice constant Ref.5. For values typical for a charge density wave regime Ref.6 we have $\epsilon \sim 10$, $\nu \sim 1$, $\Delta x \sim 1 nm$ and $U_c \sim 40 mV \sim 500 K$ so that the Aubry pinned phase should be visible at room temperature. The obtained U_c value is rather high that justifies the fact that we investigated thermoelectricity in the frame of classical mechanics of interacting electrons.

Message from Novosibirsk GES

References:

R1. A.F.Ioffe and L.S.Syil'bans, Re. Prog. Phys. **22**, 167 (1969)
R2. H.J. Goldsmid, *Introduction to thermoelectricity*, Springer, Berlin (2009).
R3. Nanoelectronics : Concepts, Theory and Modeling. Network meeting and workshop on thermoelectric transport 21-27 October 2012, Cargese, Corsica http://iramis.cea.fr/meetings/nanoctm/program.php
R4. Slides at R3 by O.Bourgeois, L.W.Molenkamp, S.Voltz
R5. I.Garcia-Mata, O.V.Zhirov, D.L.Shepelyansky, EPJD **41**, 325 (2007)
R6. S.Brazovskii *et al.*, Phys. Rev. Lett. **108**, 096801 (2012)